Electronic Structure of $Ag_5Pb_2O_6$

Theodore D. Brennan[†] and Jeremy K. Burdett*

Department of Chemistry, James Frank Institute, and NSF Center for Superconductivity, The University of Chicago, Chicago, Illinois 60637

Received December 10, 1993[⊗]

The results of tight-binding calculations on the subvalent silver-rich oxide $Ag_5Pb_2O_6$ indicate that the correct valence state formulation is $^3_\infty[Ag_5]^{4+}Pb^{4+}{}_2O^{2-}{}_6$. The odd electron per formula unit in $[Ag_5]^{4+}$ is delocalized over the entire silver substructure, namely over both the silver atoms making up the Kagomé layer and those of the chains which are threaded through it. Although this state of affairs results in a half-filled silver s band at the Fermi level, the structure does not distort to lower symmetry because of the three-dimensional nature of the Fermi surface. Both the electronic density of states and the Fermi surface, although complicated, may be readily understood as a combination of contributions from the layer and chain atoms of the silver substructure. It is suggested that doping the material with fluorine (to give $Ag_5Pb_2O_5F$) should be a good test of the half-filled band for the oxide, since filling it with one more electron should lead to a semiconductor.

Introduction

Bonding interactions between formally d^{10} centers play an important role in a number of solid-state and coordination compounds. The ability of d^{10} centers to form bonds is most clearly seen in the dimeric Pt^0 compound $[Pt(t\text{-}Bu)_2P(CH_2)_3P(t\text{-}Bu)_2]_2$, where the two platinum atoms are not bridged and have a bond length of 2.765 Å.[1] The formation of d^{10} bonding interactions in dimers and clusters has been shown to occur by the mixing of higher energy s and p functions into predominantly d-type molecular orbitals resulting in the replacement of closed-shell d^{10}–d^{10} repulsive interactions by weakly bonding interactions.[2–5] In addition to examples from coordination chemistry, many solid-state Cu, Ag, Au, Cd, and Hg compounds are known that contain metal substructures, including chains, ribbons, layers, and 3d frameworks that contain formally d^{10} metals with metal–metal distances comparable to or even shorter than those in the corresponding elemental solids.[5–7]

Among the silver compounds with Ag–Ag-bonded substructures, there is a subclass of compounds having formally subvalent (less than 1+) silver atoms and also belonging to this class of compounds. Ag_2F has an *anti*-CdI_2 structure[8] with formally $Ag^{1/2+}$. Ag_3O has[9] a distorted *anti*-BiI_3 structure with distinct $(Ag_6)^{4+}$ clusters. $Ag_6Ge_{10}P_{12}$ has a more complex structure but also contains[10] $(Ag_6)^{4+}$ clusters. The two other known subvalent silver-rich oxides are $Ag_5Pb_2O_6$,[11,12] the subject of this paper, and $Bi_4Ag_{14}O_{12}$.[13] The electronic structures of silver oxides, geometrically very different from their copper analogs, are of interest not only in their own right but also in view of the interesting properties of metal cuprates. A copper oxide sheet with an electron count close to half-filling possesses very interesting electrical properties.

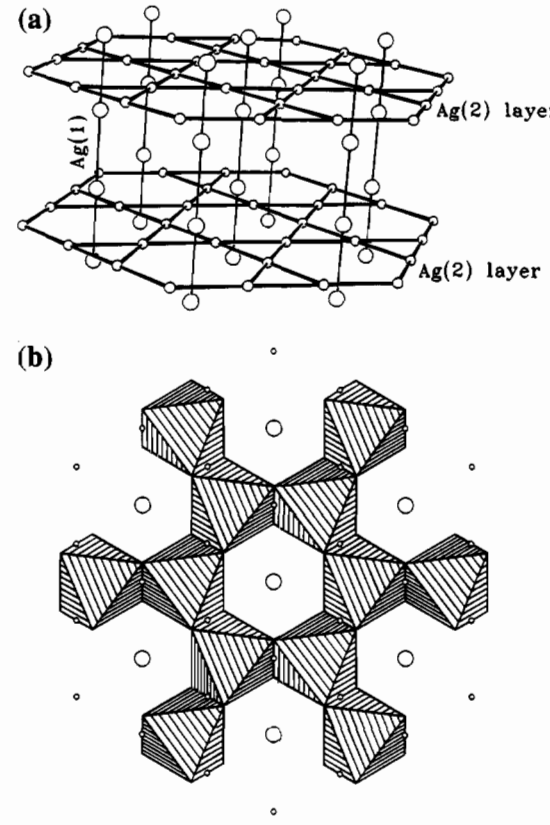

Figure 1. (a) Arrangement of the silver atoms in $Ag_5Pb_2O_6$ and (b) that of the Pb_2O_6 network. The holes in the latter are threaded by silver chains which also penetrate the Kagomé net.

The structure of $Ag_5Pb_2O_6$ was first reported by Byström and Evers[11] and later redetermined by Jansen, Bortz, and Heidebrecht.[12] The structure is an interesting one. It consists of a Ag–Ag-bonded substructure (Figure 1a) with three Ag(2) atoms

[†] Present address: Department of Chemistry, Morgan State University, Baltimore, MD 21239.

[⊗] Abstract published in *Advance ACS Abstracts,* September 1, 1994.

(1) Yoshida, T.; Yamagata, T.; Tulip, T. H.; Ibers, J. A.; Otsuka, S. *J. Am. Chem. Soc.* **1978**, *100*, 2063.
(2) Mehrotra, P. K.; Hoffmann, R. *Inorg. Chem.* **1978**, *17*, 2187.
(3) Dedieu, A.; Hoffmann, R. *J. Am. Chem. Soc.* **1978**, *100*, 2074.
(4) Jiang, Y.; Alvarez, S.; Hoffmann, R. *Inorg. Chem.* **1985**, *24*, 749.
(5) Cui, C. X.; Kertesz, M. *Inorg. Chem.* **1990**, *29*, 2568.
(6) Jansen, M. *J. Less-Common Met.* **1980**, *76*, 285.
(7) Jansen, M. *Angew. Chem., Int. Ed. Engl.* **1987**, *26*, 1098.
(8) Argay, G.; Naray-Szabo, F. *Acta Chim. Acad. Sci. Hung.* **1966**, 329.
(9) Beesk, W.; Jones, P. G.; Rumpel, H.; Schwarzmann, E.; Sheldrick, G. M. *J. Chem. Soc., Chem. Commun.* **1981**, 664.
(10) Von Schnering, H.-G.; Häusler, K.-G. *Rev. Chim. Miner.* **1976**, *13*, 71.
(11) Byström, A.; Evers, L. *Acta Chem. Scand.* **1950**, *4*, 613.
(12) Jansen, M.; Bortz, M.; Heidebrecht, K. *J. Less-Common Met.* **1990**, *161*, 17.
(13) Masse, R.; Tordjiman, I.; Durif, A. *C. R. Seances Acad. Sci., Ser. 2* **1986**, *302*, 631.

0020-1669/94/1333-4794$04.50/0

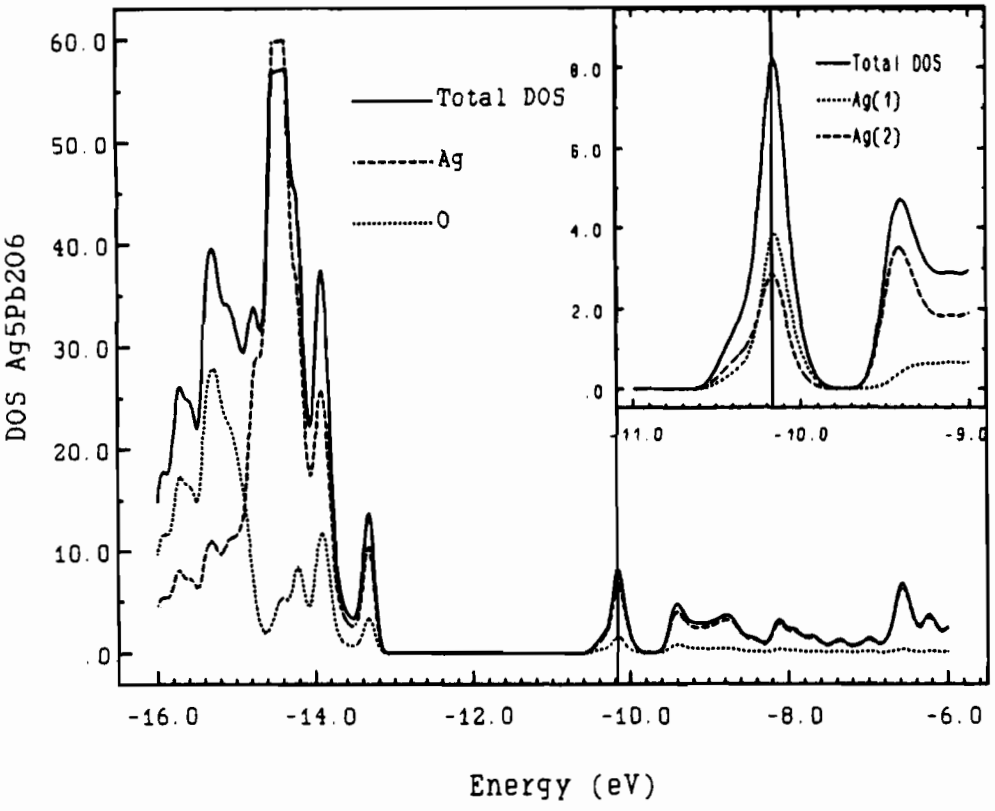

Figure 2. Density of states for $Ag_5Pb_2O_6$ with the projected silver (- - -) and O (•••) contributions. An expanded view of the −11 to −9 eV region is shown with projections showing the contributions from Ag(1) chain and Ag(2) layer atoms.

per cell arranged in a Kagomé net (3636 net) shown in **1** and two Ag(1) atoms per cell arranged in a linear chain perpendicular

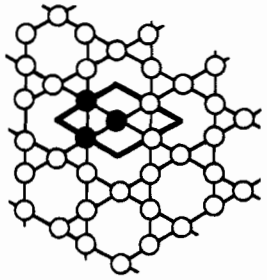

1

to the Kagomé layer with alternating long and short distances along the chain. The short Ag−Ag distances in $Ag_5Pb_2O_6$ are 3.093 and 3.317 Å along the Ag(1) chains, 3.345 Å between Ag(1) and Ag(2), and 2.966 Å within the Kagomé layers. For comparison, the Ag−Ag distance in elemental silver is 2.88 Å.[14] This interesting silver substructure interpenetrates hexagonal layers of $^2_\infty[PbO_3^{2-}]$ which contain octahedrally coordinated Pb, giving the overall formula $Ag_5Pb_2O_6$ (Figure 1b). The two different Ag−Ag distances along the chain reflect the different units they thread, the Kagomé net and the Pb_2O_6 slab. Identifying the lead as Pb^{4+} and the oxygen as O^{2-} leads to the formulation $(Ag_5)^{4+}Pb^{4+}{}_2O^{2-}{}_6$. Such a description leads to one lone s electron associated with the silver atoms and lying in a silver 5s orbital from orbital energy considerations. Byström and Evers suggested[11] that the electronic structure might be accounted for by the presence of a Ag−Ag bond between the atoms in the silver chain, $(Ag_2)^+$ $Ag^+{}_3Pb^{4+}{}_2O^{2-}{}_6$. Jansen *et al.*, on the basis of structure and conductivity measurements, suggested[12] that one electron was delocalized and described the valence state formulation as $Ag^+{}_5Pb_4{}^+{}_2O^{2-}{}_6(e^-)$. Substitution of the lead by Bi^{3+} leads[12] to a rapid increase in resistivity and the eventual generation of an insulator. Substitution by In^{3+} leads[14] though to only a small increase in resistivity. In this paper we examine the electronic structure of $Ag_5Pb_2O_6$ using the extended Hückel implementation of tight-binding theory[15,16] to examine how best to represent the valence state formulation and distribution of electrons in $Ag_5Pb_2O_6$. Although such a model has several obvious theoretical drawbacks, it is probably the best method available to tackle a system of this complexity where one wishes to understand how the electronic structure of the solid is built up.

Electronic Structure

The calculated density of states for $Ag_5Pb_2O_6$ in the region −16 to −6 eV is shown in Figure 2. The bands between −16 and −13.5 eV are the silver d bands, and as anticipated, the Fermi level (at −10.16 eV) lies in the middle of a band composed of mostly silver s character. The valence and higher energy bands are pushed up in energy by antibonding interactions with the oxygen atom orbitals, but the majority contribution to these bands comes from these silver s orbitals. The composition of the silver s band at the Fermi level is shown as a function of Ag(1) and Ag(2) character in the inset graph of Figure 2. It is almost equally composed of silver s character from both the chain (Ag(1)) and net (Ag(2)), atoms and the electron in this band is thus delocalized over both silver sites. The presence of the half-filled band and its character indicate

(14) Bortz, M.; Jansen, M.; Huhl, H.; Bucher, E. *J. Solid State Chem.* **1993**, *103*, 447.

(15) Burdett, J. K. *Prog. Solid State Chem.* **1984**, *15*, 173.
(16) Hoffmann, R. *Solids and Surfaces*; VCH Publishers: New York, 1988.

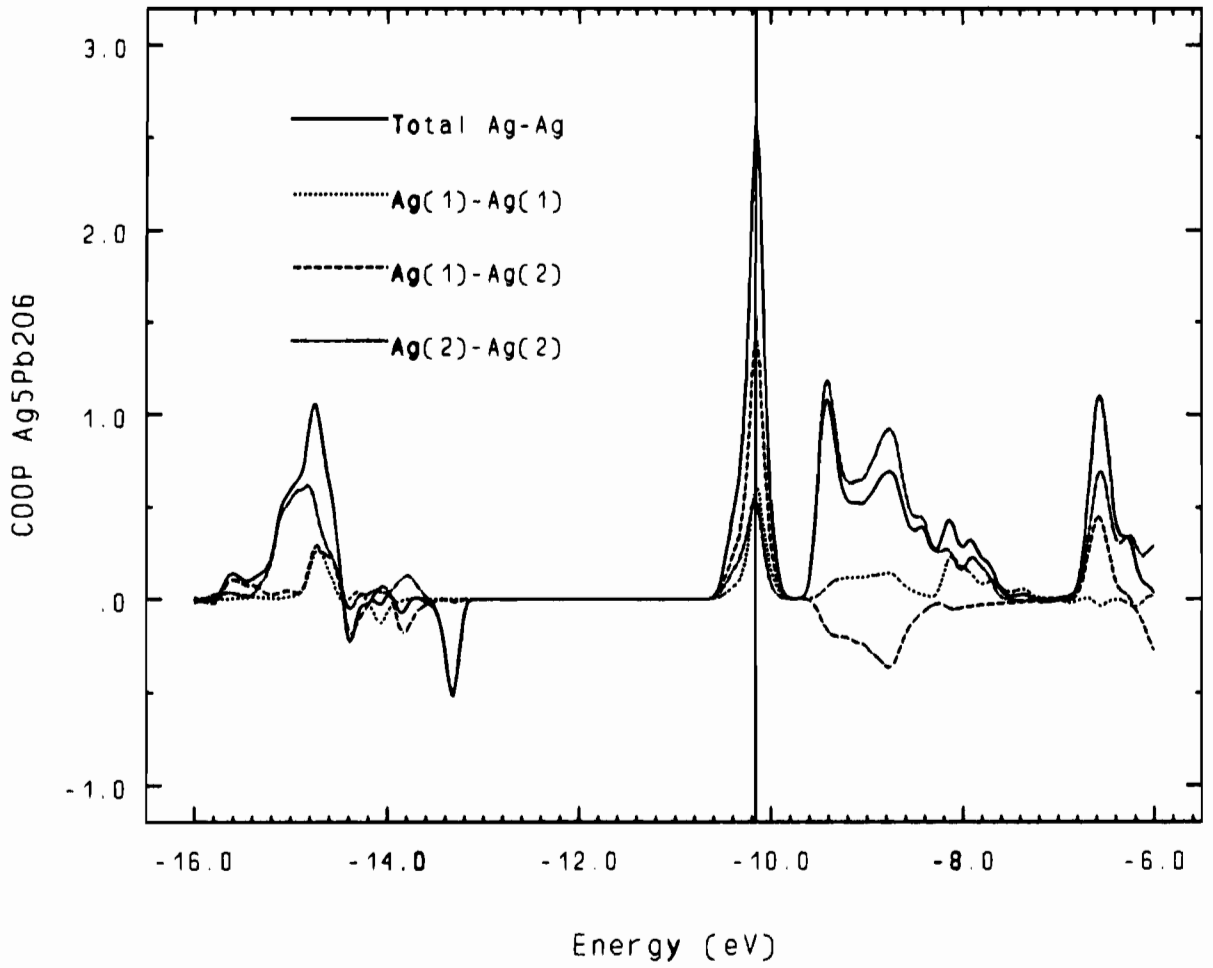

Figure 3. Ag−Ag bond orbital overlap populations (COOP) for $Ag_5Pb_2O_6$ as a function of energy: (—) total Ag−Ag overlap; (•••) Ag(1)−Ag(1) population contribution; (- - -) Ag(1)−Ag(2) layer−chain population contribution; (— • —) Ag(2)−Ag(2) overlap. As usual, a positive value indicates a bonding interaction.

a three-dimensional metal and a valence formulation for $Ag_5Pb_2O_6$ of $^3_\infty[Ag_5]^{4+}$, $Pb^{4+}{}_2$, and $O^{2-}{}_6$. It also removes the question of the structural stability of a compound with a half-filled band, since the dimensionality is greater than 1.

The bond overlap population (COOP) curve is shown in Figure 3. The Ag−Ag antibonding component in the silver d-band region has been depressed due to d−s−p mixing, which leads in the band model to an understanding of the ability to form d^{10}−d^{10} bonds.[2-5] This is shown in a pictorial way in **2**.

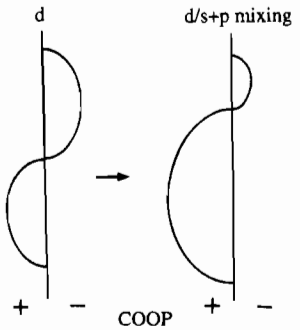

2

In the absence of such mixing the "d band" will be bonding at the bottom and antibonding at the top. Stabilization of all of the levels by admixture of silver 5s and 5p orbitals increases the strength of the bonding component and decreases the strength of the antibonding component, leading overall to a positive total metal−metal overlap population for the d^{10} configuration. This is the solid-state analog of the electronic situation in the Pt dimers noted above.

Notice that the results of Figures 2 and 3 lead to a trio of valence and conduction bands (**3**). The deepest (half-occupied)

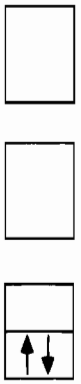

3

and highest in energy both contain Ag(1) (chain) and Ag(2) (net) character, but the middle band is virtually only associated with the Ag(2) atoms of the Kagomé net. The lowest energy of the trio, the silver s band at the Fermi level, is bonding with respect to Ag−Ag interactions, and any electrons added to this

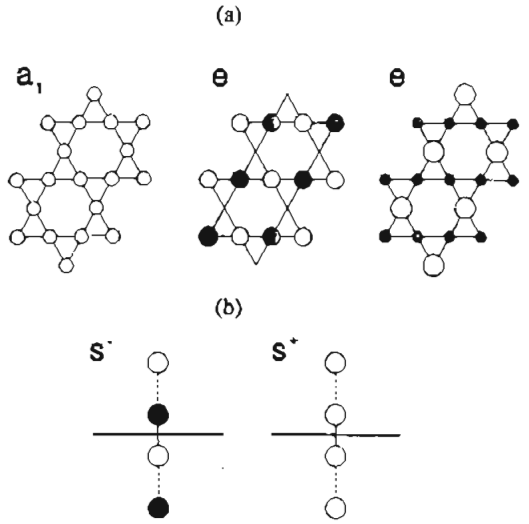

Figure 4. (a) a_1' and e′ levels of the 5s orbitals of the Ag_3 triangle. (b) Symmetric and antisymmetric combinations of chain Ag 5s orbitals which cap the Kagomé net.

band will further enhance Ag−Ag bonding in the silversub-structure. Although not shown, but already noted, the silver s band at the Fermi level also has some Ag−O antibonding character. Of particular interest is how the rather simple band structure of **3** results.

Since the energy levels of interest are largely silver in character, it is quite legitimate to examine the electronic structure of the Kagomé net itself and how the band structure of the complete silver structure is derived from it. This net has already been viewed in electronic terms;[17] it appears as the building block of several structures including those of the Laves phases. For the situation here, the band structure should be especially simple since each silver atom carries a single 5s orbital. One way of envisioning the Kagomé net which is useful in deriving its electronic structure is clear from **1**. The net consists of triangles of atoms whose centroid is located at the $^1/_3$, $^1/_3$ site of a primitive hexagonal cell. Each triangle has six equidistant neighbors. The simplest picture of the electronic structure of the solid is thus one which is derived from the extended behavior of the a_1' and e′ levels of the isolated triangle. These are shown in Figure 4a, and their behavior with **k** is readily derived within the Hückel model.[17] At Γ, the zone center, where the orbitals of the atoms contained within the unit cell are all in-phase with their neighbors, the energy of the "a_1'" band is just $\alpha + 2\beta + 2\beta = \alpha + 4\beta$ and that of the "e" band $\alpha - \beta - \beta = \alpha - 2\beta$. Away from Γ, the bands may interact at general points in **k** space, and these labels are not of universal validity, just as for the π and π^* bands of graphite,[14] but the picture, **4**, is still a

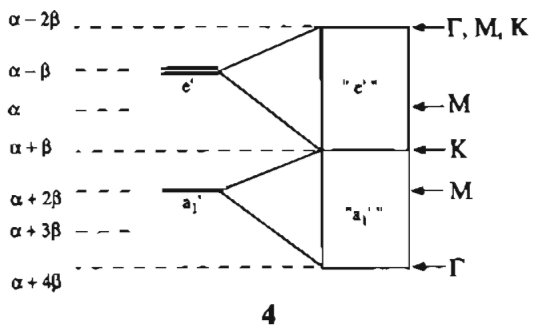

4

(17) Johnson, R. L.; Hoffmann, R. *Polyhedron* **1990**, *9*, 1901.

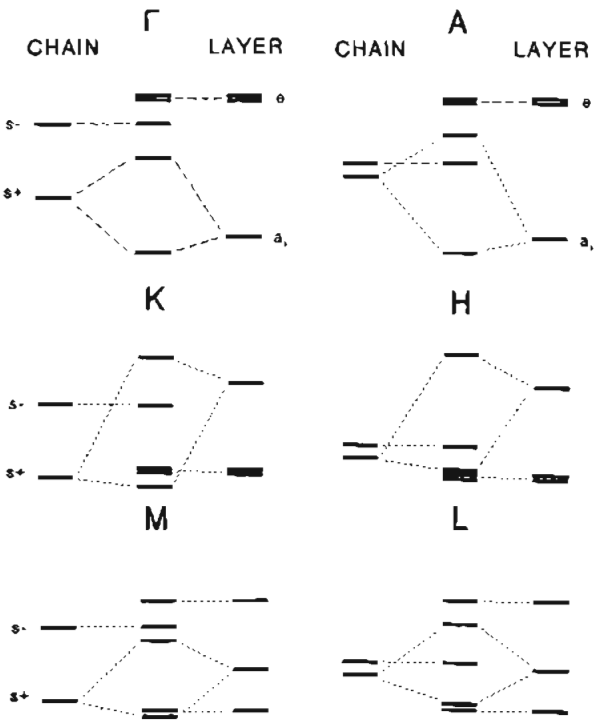

Figure 5. Assembly of the band structure of the capped Kagomé net at various k points from the energy bands (**4**) of the net and the levels (Figure 4b) of the capping atoms.

useful one. The bands touch at point K. The important ingredient is the presence of the lower-lying "a_1'" band. The 5s orbitals of the one-dimensional chain which is threaded through the Kagomé net are of course cylindrically symmetrical. Hence at Γ they will not interact with the "e′" orbitals of the net at all but will interact with the "a_1'" orbitals at all points in the zone. This is a simplified picture of course. Away from Γ, there will be a nonzero interaction between these chain orbitals and the "e′" orbitals of the net. The general picture is shown in Figure 5 at six symmetry points in the zone. Rather than using energy bands of such a chain, we take advantage of the alternating Ag−Ag distances (≈3.0 and 3.3 Å) to cap the chain on either side with a silver atom. Thus the two silver 5s levels are either symmetric (s^+) or antisymmetric (s^-) with respect to the plane (Figure 4b). Only the former can interact with the layer s levels by symmetry. The bottom and top orbitals of the trio of **3** are just the in- and out-of-phase combinations of chain and net bands. They have approximately equal contributions from Ag(1) and Ag(2) and in the lower energy band of the pair are bonding between Ag(1) and Ag(2), between Ag(1) and Ag(1), and between Ag(2) and Ag(2), as revealed by the full band structure calculations of Figures 2 and 3. The middle band of the trio is largely located on the Ag(2) atoms of the layer. The origin of a half-filled band of a solid with this composition and structure is thus now quite clear. Addition of an electron should fill this band and lead to an insulator, as should removal of this electron. This latter result has been achieved by substitution of half of the Pb^{4+} with Bi^{3+},[14] although the substitution experiment with indium led to little change in resistivity.

The computed band structure for the half-occupied band of $Ag_5Pb_2O_6$ is shown in Figure 6, along selected directions in the Brillouin zone in the energy region near the Fermi level. The half-filled band identified for the capped Kagomé net of silver atoms is preserved but its dispersion behavior perturbed

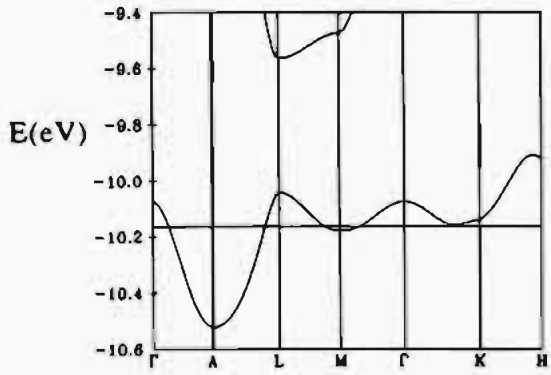

Figure 6. Band structure diagram for $Ag_5Pb_2O_6$ shown along various directions in reciprocal space. The Fermi energy is shown by the solid horizontal line at −10.16 eV.

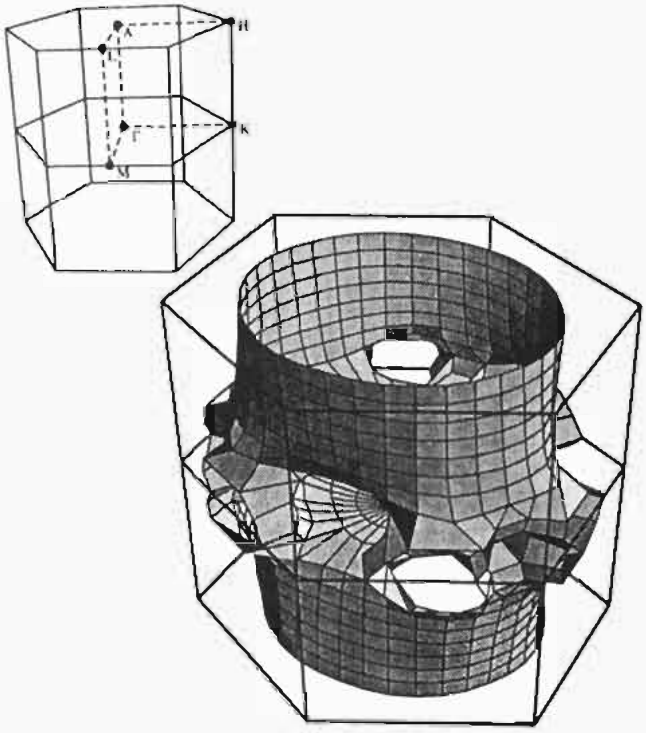

Figure 7. Three-dimensional view of the Fermi surface of $Ag_5Pb_2O_6$. The silver s band crossing the Fermi level is below E_F at M and A and above at Γ, K, H, and L.

by the presence of the lead and oxide ions. This band is filled at A and M but empty at points Γ, K, L, and H. Because the silver s band at the Fermi level is bonding with respect to Ag−Ag interactions, the zone center, Γ, might be expected to be below E_F. However, due to mixing with lead and oxygen orbitals, the band is pushed above E_F at the zone center. The detailed electronic description is somewhat complicated and involves the balance between three different types of Ag−Ag interactions and the Ag−O and Pb−O interactions. The last two contributions, although giving rise to a band of mixed character, do not change the basic description of the half-filled, largely silver band.

With a half-filled band and high symmetry, one might expect $Ag_5Pb_2O_6$ to be unstable relative to some distorted form, although we have noted already a dimensionality greater than 1. To understand the stability further, one has to look at the Fermi surface,[18] shown in Figure 7. The Fermi surface was

(18) Canadell, E.; Whangbo, M.-H.; *Chem. Rev.* **1991**, *91*, 965.

Table 1. Atomic Parameters

orbital	ζ_1	c_1	ζ_2	c_2	H_{ii}
Ag 5s	2.244				−11.16
Ag 5p	2.202				−5.81
Ag 4d	6.07	0.5591	2.663	0.6048	−14.54
Pb 6s	2.35				−15.7
Pb 6p	2.06				−8.0
O 2s	2.275				−32.3
O 2p	2.275				−14.8

plotted using 10 slices from $z = 0$ to $\pi/2$ with 441 points per slice. Bicubic spline interpolation within each slice was used to locate the Fermi surface, and the surface was plotted using Mathematica. In cases where structural or electronic distortions occur, they can be understood by "nesting" of the Fermi surface.[18] The Fermi surface is clearly three-dimensional in nature and does not allow for any nesting which would lead to a structural or electronic distortion. The Fermi surface is approximately cylindrical with projections out the M direction of the Brillouin zone. As noted from the band structure, in the area around the zone center the silver s band lies above the Fermi level.

We noted earlier the approximately equal contributions from the 5s orbitals located on chain and net atoms at the Fermi level. The odd electron is thus distributed in the ratio of 2:3 over the two types of atoms. It is interesting to see how Fermi surface calculations for the two systems, $[Ag_3Pb_2O_6]^{1.6-}$ with no silver chain atoms and $[Ag_2Pb_2O_6]^{2.4-}$ with no silver layer atoms, show how this apparently complicated Fermi surface can be simply understood as a combination of contributions from the two types of silver atoms. Ignore the Pb_2O_6 layers for the time being. The Fermi surface of a partially filled layer would be a cylinder (Figure 8a), and the Fermi surface for a partially filled one-dimensional chain would be a slab (Figure 8b). The overall shape of the Fermi surface (Figure 8c) can be understood as a cylindrical component due to the two-dimensional Ag(2) layers and the projections in the $\mathbf{k} = (x, y, 0)$ plane due to the one-dimensional Ag(1) chains. As mentioned before, antibonding interactions between silver and O lead to Γ and K being pushed above the Fermi level, leading to the Fermi surface for the complete oxide of Figure 7.

Discussion

Generation of the electronic density of states for $Ag_5Pb_2O_6$ shows that the correct valence description for the compound is $^3_\infty[Ag_5]^{4+}Pb^{4+}{}_2O^{2-}{}_6$ and that the Fermi level lies in a half-filled band of mostly silver s character contributed almost equally by chain and Kagomé net silver atoms. In spite of the half-filled band, the structure does not distort to lower symmetry because of the three-dimensional nature of the Fermi surface. Both the density of states and the Fermi surface can be readily understood as a combination of the two parts of the metal−metal-bonded substructure. Because the band at the Fermi level is half-filled, and bonding everywhere between the silver atoms, filling the band with electrons should enhance the bonding within the silver substructure. The full band should also dramatically modify the conductivity, and a semiconductor should result. Doping the structure with fluorine should be a good experimental test of the half-filled band for the oxide, since it is filled with one more electron in the material with a stoichiometry $Ag_5Pb_2O_5F$. The half-filled band for $Ag_5Pb_2O_6$ suggests immediate comparisons with the cuprate superconductors. However, although

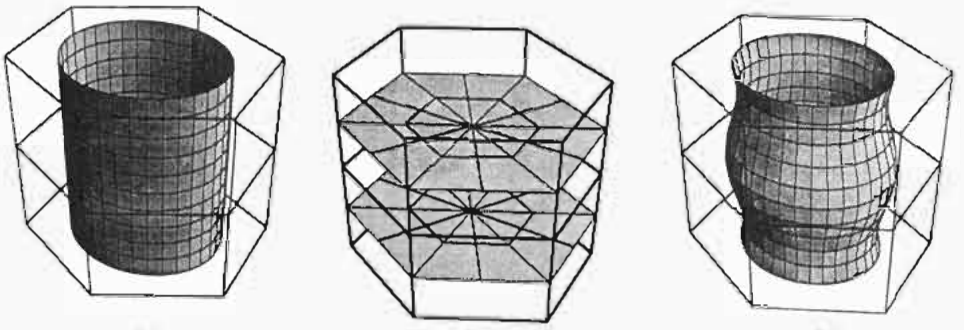

Figure 8. Fermi surfaces of the partial structures (a) $[Ag_3Pb_2O_6]^{1.6-}$ with no silver chain atoms and (b) $[Ag_2Pb_2O_6]^{2.4-}$ with no silver layer atoms and the complete structure (c) $Ag_5Pb_2O_6$. (The Pb_2O_6 substructure is not included in the calculations.)

the bandwidth may be comparable to that in those systems, the much smaller electron−electron interactions for the second-row metal Ag lead to a metal for the half-filled system, in contrast to the insulating state for the cuprate. Nature, however, is often full of surprises, and the metal−insulator transition generated by doping should perhaps be studied further.

Acknowledgment. We thank Dr. Enric Canadell for his advice concerning Fermi surfaces. This research was supported by the National Science Foundation under Grant DMR-88-09854.

Appendix

The H_{ii} and Slater parameters (listed in Table 1) for Pb and O were taken from standard collections,[19] and those for silver were the same as those used in ref 5. The extended-Hückel-based[20] tight-binding calculations were performed using the program EHMACC.[21]

(19) Alvarez, S. Unpublished collection of EHMO parameters.
(20) (a) Hoffmann, R. *J. Chem. Phys.* **1963**, *39*, 1397. (b) Hoffmann, R.; Lipscomb, W. N. *J. Chem. Phys.* **1962**, *36*, 2179, 3489; **1962**, *37*, 2872.
(21) The program EHMACC was written by M.-H. Whangbo, M. Evain, T. Hughbanks, M. Kertesz, S. Wijeyesekera, C. Wilker, C. Zheng, and R. Hoffmann.